Draft version November 9, 2006
Preprint typeset using LaTeX style emulateapj v. 6/22/04

THE POWER SPECTRUM OF SUPERSONIC TURBULENCE IN PERSEUS

Paolo Padoan[1], Mika Juvela[2], Alexei Kritsuk[1] and Michael L. Norman[1]

Draft version November 9, 2006

ABSTRACT

We test a method of estimating the power spectrum of turbulence in molecular clouds based on the comparison of power spectra of integrated intensity maps and single-velocity-channel maps, suggested by Lazarian and Pogosyan. We use synthetic ^{13}CO data from non-LTE radiative transfer calculations based on density and velocity fields of a simulation of supersonic hydrodynamic turbulence. We find that the method yields the correct power spectrum with good accuracy. We then apply the method to the Five College Radio Astronomy Observatory ^{13}CO map of the Perseus region, from the COMPLETE website. We find a power law power spectrum with slope $\beta = 1.81 \pm 0.10$. The values of β as a function of velocity resolution are also confirmed using the lower resolution map of the same region obtained with the AT&T Bell Laboratories antenna. Because of its small uncertainty, this result provides a useful constraint for numerical codes used to simulate molecular cloud turbulence.

Subject headings: ISM: clouds – ISM: kinematics and dynamics – ISM: structure

1. INTRODUCTION

The large scale dynamics of interstellar clouds is characterized by random supersonic motions with a very large Reynolds number, meaning that inertia is much larger than viscous forces. This interstellar turbulence is a dominant transport mechanism in many astrophysical processes and plays an important role in the fragmentation of star-forming clouds. Random supersonic flows in molecular clouds result in a complex network of highly radiative shocks causing very large density contrasts and shaping the clouds into the observed self-similar filamentary structure (Nordlund & Padoan 2003).

Our understanding of turbulence is limited by the lack of general analytical solutions of the Navier-Stokes equation. Statistical properties of turbulence, essential to modeling many astrophysical processes, are therefore derived almost entirely from numerical simulations. In the case of incompressible hydrodynamic turbulence, numerical simulations can be compared with laboratory experiments. This is not possible for the isothermal, supersonic, magneto-hydrodynamic (MHD) turbulence regime of molecular clouds. The best approach to validate numerical models is in this case a statistical comparison of observational data with *synthetic data* from numerical simulations.

Padoan et al. (2004) found that the exponents of the velocity structure functions of compressible and super-Alfvénic turbulence follow a generalized She-Lévêque scaling (Boldyrev 2002), depending only on the rms Mach number of the flow. Based on that scaling formula, if one of the exponents is known (for example the second order that corresponds to the velocity power spectrum) all the others can be derived, up to some order. While the scaling formula is well constrained numerically, its normalization, given by the actual value of one of the exponents, is harder to measure and may depend on the numerical method used to simulate the turbulence.

Numerical simulations of supersonic hydrodynamic (HD) and magneto-hydrodynamic (MHD) turbulence have yielded a range of values of the slope of the velocity power spectrum, from the Kolmogorov value of $\beta = 5/3$, to the Burgers value of $\beta = 2$ (Frisch & Bec 2001), and beyond. The main problems with the numerical estimate of the power spectrum are i) The limited extent in wavenumbers of the inertial range of turbulence, or even its complete absence in the case of low resolution (or highly dissipative) simulations; ii) The emergence of the bottleneck effect (e.g. Falkovich 1994; Dobler et al. 2003; Haugen & Brandenburg 2004) as soon as the numerical resolution is large enough to generate an inertial range; iii) The dependence of the power spectrum on the numerical schemes used to stabilize the shocks; iv) The dependence of the numerical resolution necessary for convergence on the numerical method. Given these difficulties, reliable measurements from interstellar clouds provide useful constraints to validate numerical models and to improve our knowledge of supersonic turbulence.

Lazarian & Pogosyan (2000) have demonstrated that the exponent of the velocity power spectrum can in principle be derived from spectral maps of emission lines by comparing the power spectrum of integrated intensity with the power spectrum of single-velocity-channel intensity. Their method was tested with numerical simulations of turbulent flows, where the velocity and density fields had to be modified to generate power law power spectra, due to the limited numerical resolution (Esquivel et al. 2003). In this Letter we present a new test of their method. Thanks to the high numerical resolution of our simulation ($1,024^3$ computational zones), our density and velocity power spectra exhibit extended power laws, and no modifications to the original turbulent fields are required. Furthermore, the method is tested by computing synthetic CO emission lines with a non-LTE radiative transfer code. We find the method allows to retrieve the power law exponent of the velocity power spectrum with good accuracy, using the J=1-0 ^{13}CO line. We then apply the method to the Five College Radioastronomy Observatory (FCRAO) survey of the Perseus molecular

[1] Department of Physics, University of California, San Diego, CASS/UCSD 0424, 9500 Gilman Drive, La Jolla, CA 92093-0424; ppadoan@ucsd.edu
[2] Department of Astronomy, University of Helsinki, Tähtitorninmäki, P.O.Box 14,FI-00014 University of Helsinki, Finland

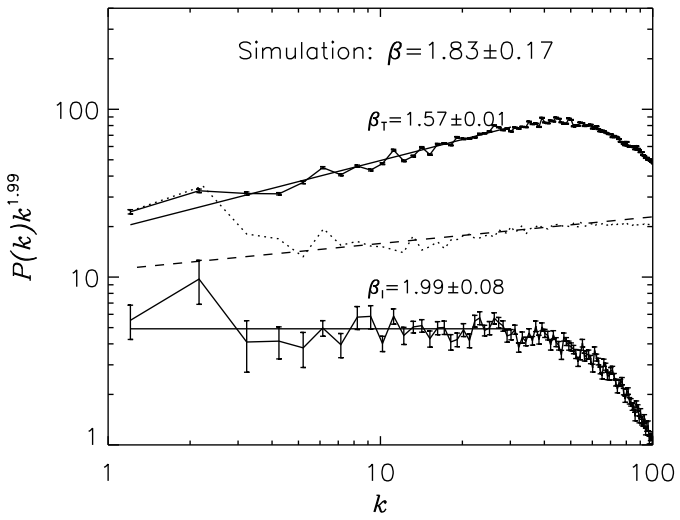

FIG. 1.— Compensated power spectrum of integrated intensity (bottom curve) and average of the compensated power spectra of single-velocity-channel intensity maps (top curve) from the numerical simulation. The dotted plot (middle curve) is the 3D power spectrum of velocity and the dashed line shows the $\beta = 1.83$ slope predicted by the method.

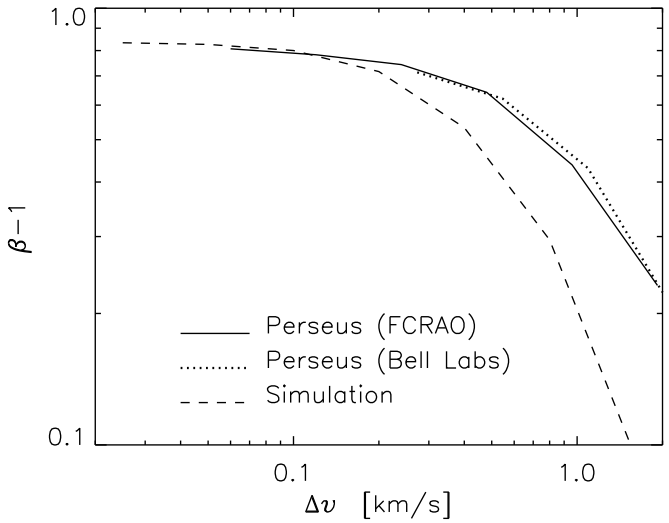

FIG. 2.— Convergence plot for the exponent of the velocity power spectrum as a function of the channel width.

cloud complex (Ridge et al. 2006), publicly available from the COMPLETE website, and estimate the power spectrum exponent $\beta = 1.81 \pm 0.10$. The result is confirmed by the analysis of the lower resolution map of the same region obtained with the AT&T Bell Laboratories antenna (see Padoan et al. 1999).

2. SYNTHETIC SPECTRAL MAPS

Synthetic maps of the J=1-0 line of ^{13}CO are computed with a new non-LTE radiative transfer code that has been extensively tested against the older Monte Carlo code (Juvela 1997). As a model of the density and velocity fields in interstellar clouds we use the results of a supersonic simulation of HD turbulence with rms Mach number $M = 6$. Our purpose is not to simulate the conditions found in a specific molecular cloud, but rather to test a general method of estimating the velocity power spectrum. We will study the effect of different parameter values elsewhere. Because the method is based on an analytical derivation by Lazarian & Pogosyan (2000) that neglects correlations between density and velocity, we expect it to work equally well for a vast range of turbulence parameters.

The simulations are carried out with the *Enzo* code, developed at the Laboratory for Computational Astrophysics by Bryan, Norman and collaborators (Norman & Bryan 1999). *Enzo* is a public domain Eulerian grid-based code (see http://cosmos.ucsd.edu/enzo/) that adopts the Piecewise Parabolic Method (PPM) of Colella & Woodward (1984). We use an isothermal equation of state, periodic boundary conditions, initially uniform density and initial random large scale velocity. The turbulence is forced in Fourier space only in the wavenumber range $1 \leq k \leq 2$, where $k = 1$ corresponds to the size of the computational domain that contains $1,024^3$ computational zones (for details see Kritsuk et al. 2006).

The radiative transfer calculations assume a box size of 5 pc, a mean density of 10^3 cm^{-3}, a mean kinetic temperature of 10 K, an rms Mach number $M = 6$ (consistent with the HD simulation) and a uniform abundance of ^{13}CO molecules. These values were chosen as a generic reference model, not tailored to the Perseus molecular cloud complex. The original density and velocity data-cubes are re-sampled to a resolution of 256^3 zones. This has three advantages: i) It leaves density and velocity fields with power spectra that are power laws almost up to the new Nyquist frequency; ii) It speeds up enormously the radiative transfer calculations; iii) It generates a map of synthetic spectra with a range of scales comparable to that of the rebinned FCRAO map of Perseus (see below).

The result of the radiative transfer calculations is a map of spectral profiles of the line intensity, $T(v, \mathbf{x})$, over 280 velocity channels, v, and across all positions, $\mathbf{x}$, within the map of 256^2 positions. The sum of the line intensity of all velocity channels, multiplied by the channel width, $\Delta v = 0.025$ km/s, gives the integrated intensity at each position, $I(\mathbf{x}) = \Sigma_v T(v, \mathbf{x})\, \Delta v$. The map $I(\mathbf{x})$ may be used to derive a rough estimate of the column density. We do not address the issue of converting integrated intensities into accurate estimates of column density, because we derive the velocity power spectrum directly from the line intensity data.

3. THE METHOD

We call $P_{\rm I}(k)$ the two-dimensional spatial power spectrum of the integrated intensity map, $I(\mathbf{x})$, and look for a power law fit such that, $P_{\rm I}(k) \propto k^{-\beta_{\rm I}}$. The integrated map is the sum of all the single-velocity-channel maps. We then call $P_{\rm T}(v, k)$ the two-dimensional spatial power spectrum of the individual channel maps, $T(v, \mathbf{x})$, where we have left the velocity dependence to stress that there are as many of these maps and power spectra as there are velocity channels. We look for a power law fit to the average of these power spectra as well, such that $P_{\rm T}(k) = \langle P_{\rm T}(v, k) \rangle_v \propto k^{-\beta_{\rm T}}$. Finally, we assume the three dimensional spatial power spectrum of the velocity

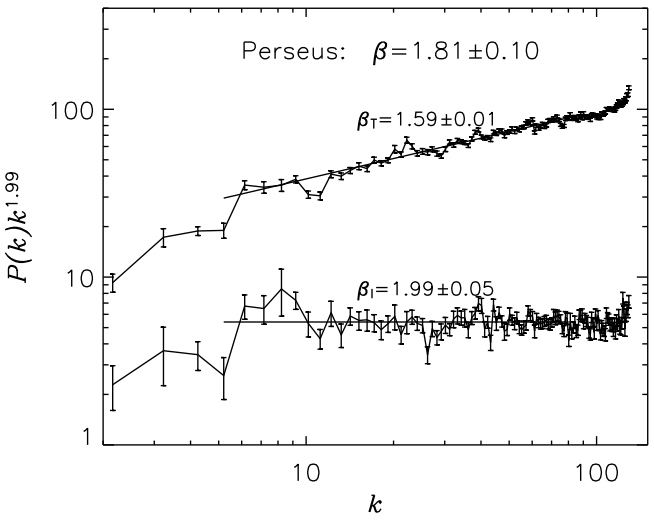

FIG. 3.— Same as in Figure 1, but for the FCRAO survey of Perseus (Ridge et al. 2006).

field is also a power law (a reasonable assumption for the cloud turbulence, given the huge Reynolds number), $P_{\rm v}(k) \propto k^{-\beta}$.

The result of Lazarian & Pogosyan (2000) can be expressed as $\beta = 1 + 2(\beta_{\rm I} - \beta_{\rm T})$, if $\beta_{\rm I} < 2$, and $\beta = 1 + 2(2 - \beta_{\rm T})$, if $\beta_{\rm I} > 2$. In this Letter we test their result only for the case of $\beta_{\rm I} < 2$. The single-velocity-channel power spectra are shallower than the integrated intensity power spectrum, $\beta_{\rm T} < \beta_{\rm I}$, because they contain small-scale structure originating from both the density and the velocity fields. It is this difference that makes it possible to derive the velocity power spectrum exponent, based on the above formula.

In this Letter we refer to power spectra as the *total* power within shells of wavenumber between k and $k+dk$. In Lazarian & Pogosyan (2000), the power spectra are defined as the *average* power within shells of wavenumber between k and $k + dk$. Furthermore, we do not absorb the negative sign in the definition of β_I as they do. Our exponents are related to their n and m exponents in the following way: $\beta_I = 1-n$, $\beta = 1+m$. In our convention, the velocity power spectrum corresponds to the usual turbulent energy spectrum, for example $k^{-5/3}$ for the Kolmogorov case.

Fig. 1 shows $P_{\rm I}(k)$ (bottom plot) and $P_{\rm T}(k)$ (top plot) for the simulated data-cube "observed" along the x direction. The error bars are one standard deviation above and below the mean values and depend on the statistical sample size (number of Fourier modes inside each wavenumber shell), so they decrease with increasing wavenumber. The linear least square fits, plotted as solid lines, are computed in the wavenumber range $1 \le k \le 30$. Based on the estimated exponents of these two power spectra, we obtain $\beta = 1 + 2(\beta_{\rm I} - \beta_{\rm T}) = 1.83 \pm 0.17$. Values of β from synthetic maps of the data-cube observed in different directions fall within the estimated 1-σ uncertainty. The value of the velocity power spectrum exponent, computed directly from the original three dimensional velocity field, is $\beta = 1.8 \pm 0.1$ (dotted plot in Fig. 1), showing that the method retrieves the correct exponent.

In order to verify the dependence of β on the velocity channel width, we have applied the method to synthetic maps at different velocity resolutions. The result, plotted in Fig. 2, shows that the value of β is completely converged only for a channel width of the order of the thermal width. This was to be expected, because all velocity fluctuations above the thermal width may in principle affect the velocity power spectra of the single-velocity-channel maps.

This method is based on an analytical derivation by Lazarian & Pogosyan (2000) that neglects the correlations of density and velocity in turbulent flows. We interpret this test as a confirmation of the validity of their method in the case of $\beta_{\rm I} < 2$, rather than as an empirical calibration of the value of β based on $\beta_{\rm I}$ and $\beta_{\rm T}$. The uncertainty of the method, when applied to observational data, is then determined by the error bars of the observational power spectra, independently of the uncertainty of our numerical test. The final error bar is dominated by the uncertainty in the power spectrum exponent of the integrated intensity, because the uncertainty in the single-velocity-channel spectrum is reduced by averaging the power spectra of many velocity channels.

4. THE POWER SPECTRUM OF PERSEUS

We have applied the method to the J=1-0 ^{13}CO survey of the Perseus molecular cloud complex carried out with the FCRAO 14 m antenna by Ridge et al. (2006). The grid spacing of the survey is 23", and the beam size 46". The velocity-channel size is 0.06 km/s. The power spectra we compute are corrected for the effect of beam and noise, by simply dividing by the power spectrum of a gaussian beam, and subtracting the power spectrum of the noise. Spatial correlations in the noise arising from the "On-the-Fly" mapping mode are neglected. At the largest wavenumbers, the power spectra are sensitive to the noise subtraction, and realistic error bars accounting for that would make such wavenumbers essentially useless for estimating the power spectra. We therefore prefer to regrid the map to a resolution of 92", which has the advantage of increasing the signal-to-noise by a factor of 4.

The power spectra are shown in Fig. 3. The least square fits are computed in the range $5 \le k \le 80$, and yield $\beta = 1.81 \pm 0.10$. Although this range is less extended than that used with the synthetic data, it includes larger wavenumbers (between $k = 30$ and $k = 80$) than the synthetic fit (the synthetic power spectra are still affected by numerical dissipation at large wavenumbers even after rebinning from $1,024^3$ to 256^3). This reduces the final uncertainty, because the statistical sample size is much larger at larger wavenumbers ($\propto k\,dk$ in two dimensions). As a result, the 1-σ uncertainty of β is 9% for the synthetic data, and 5% for the observations.

The value of the slope of the projected density power spectrum, $\beta_{\rm I} = 1.99 \pm 0.05$ is similar to values previously found in different regions observed in HI (e.g. Green 1993; Stanimirovich et al. 1999) and CO (e.g. Bensch, Stutzki, Ossenkopf 2001; Padoan et al. 2004a). Notice that in those previous works, with the exception of Padoan et al. (2004a), the power spectrum is not integrated over wavenumber shells, so its slope is equivalent to $\beta_{\rm I} + 1$. Furthermore, the power spectrum of the ^{13}CO

integrated intensity is slightly steeper than the gas density power spectrum due to radiative transfer effects. Accounting for such effects, the slope of the projected gas density power spectrum in the Perseus region was estimated to be consistent with that of super-Alfénic turbulence simulations (Padoan et al. 2004a).

The value of β estimated for the Perseus region as a function of the velocity resolution is shown in Fig. 2 (solid line). The channel width of 0.06 km/s is close to the thermal line width and the value of β seems to be almost converged, at least within its 1-σ uncertainty. As an independent test, we have applied the method also to the AT&T Bell Laboratories map of the same region (see Padoan et al. 1999). The Bell Laboratories 7 m antenna has a beam twice the size of the FCRAO 14 m antenna. We did not regrid this map to a lower resolution, so the map resolution and size are comparable to those of the FCRAO map, but its velocity resolution is only 0.273 km/s, so it is not expected to yield a converged value of β. The values of β for the Bell Laboratories map is shown in Fig. 2 as a dotted line, showing very good agreement with the FCRAO result, well within the estimated 1-σ uncertainty.

5. DISCUSSION AND CONCLUSIONS

This result has very interesting implications. First, numerical simulations giving power spectra with slope significantly larger than $\beta = 1.8 \pm 0.1$ may be ruled out as correct descriptions of molecular cloud turbulence (at least for the Perseus region). Burgers exponent, $\beta = 2.0$, is 2σ larger than the Perseus exponent (assuming this is converged as a function of velocity resolution). The slope of the power spectra of the SPH simulations in Ballesteros-Paredes et al. (2006), $\beta \approx 2.7$ in the case of a turbulence rms Mach number ≈ 6, is 9σ larger than the present estimate, and their grid based simulations have $\beta \approx 2.2$, 4σ too large. Second, we can now derive the absolute values of the velocity structure function exponents in Perseus. Padoan et al. (2004b) have determined numerically the relative values of those exponents, so the knowledge of one of them, for example the second order exponent given by $\beta - 1$, allows to determine the absolute values of all the others.

A different method of estimating the scaling of the turbulence from molecular clouds surveys was developed by Brunt & Heyer (2002a,b), based on the principle component analysis (PCA). They analyzed 23 molecular clouds in the outer Galaxy and estimated a value $\beta = 2.2 \pm 0.3$, if the structure function exponents of order p are assumed to scale linearly as $p/3$. This value is significantly larger than the one we estimate in Perseus. However, the PCA method is dependent on a calibration with numerical simulations. Based on such a calibration, it appears that the PCA method estimates the exponent of the velocity structure functions of order $p = 0.5$ or lower (Brunt et al. 2003). Taking this into consideration, the result of Brunt & Heyer (2002b) would be roughly consistent with ours, if a very intermittent scaling of the structure function is assumed, consistent with numerical simulations of supersonic turbulence.

We have shown in this Letter that the method for estimating the velocity power spectrum slope proposed by Lazarian and Pogosyan (2000) works well in the case of $\beta_{\rm I} < 2$, and for a velocity resolution not much larger than the thermal line width. However, regions with lower turbulence Mach number than Perseus, for example the Taurus region, may have steeper density power spectra, and hence $\beta_{\rm I} > 2$. Such regions will be studied in a future work, where the method will be tested also with numerical simulations generating synthetic data with $\beta_{\rm I} > 2$.

P.P., A.K., and M.L.N. were partially supported by the NASA ATP grant NNG056601G, the NSF grants AST-0507768 and AST-0607675 and the NRAC allocation MCA098020S. We utilized computing resources provided by the San Diego Supercomputer Center and by the National Center for Supercomputing Applications. M.J. was supported by the Academy of Finland Grants no. 206049 and 107701.

REFERENCES

Bensch, F., Stutzki, J., & Ossenkopf, V. 2001, A&A, 366, 636
Boldyrev, S. 2002, ApJ, 569, 841
Brunt, C. M. & Heyer, M. H. 2002a, ApJ, 566, 276
Brunt, C. M. & Heyer, M. H. 2002b, ApJ, 566, 289
Brunt, C. M., Heyer, M. H., Vázquez-Semadeni, E., & Pichardo, B. 2003, ApJ, 595, 824
Colella, P., & Woodward, P. R. 1984, Journal of Computational Physics, 54, 174
Dobler, W., Haugen, N. E., Yousef, T. A., & Brandenburg, A. 2003, Phys. Rev. E, 68, 026304
Esquivel, A., Lazarian, A., Pogosyan, D., & Cho, J. 2003, MNRAS, 342, 325
Falkovich, G. 1994, Physics of Fluids, 6, 1411
Frisch, U., & Bec, J. 2001, New trends in turbulence. Editors: M. Lesieur, A. Yaglom, F. David, Les Houches Summer School, vol. 74, p.341, 341
Green, D. A. 1993, MNRAS, 262, 327
Haugen, N. E., & Brandenburg, A. 2004, Phys. Rev. E, 70, 026405
Juvela, M. 1997, A&A, 322, 943
Klein, R. I., Inutsuka, S., Padoan, P., & Tomisaka, K. 2006, in Protostars and Planets V, eds. B. Reipurth et al.
Kritsuk, A. G., Wagner, R., Norman, M. L., & Padoan, P. 2006, in ASP Conf. Ser., Calspace-IGPP Conf. on Numerical Modeling of Space Plasma Flows (San Francisco: ASP), in press
Lazarian, A., & Pogosyan, D. 2000, ApJ, 537, 720
Mizuno, A., Onishi, T., Yonekura, Y., Nagahama, T., Ogawa, H., & Fukui, Y. 1995, ApJ, 445, L161
Nordlund, Å., & Padoan, P. 2003, LNP Vol. 614: Turbulence and Magnetic Fields in Astrophysics, 614, 271
Norman, M. L., & Bryan, G. L. 1999, ASSL Vol. 240: Numerical Astrophysics, 19
Padoan, P., Bally, J., Billawala, Y., Juvela, M., & Nordlund, Å. 1999, ApJ, 525, 318
Padoan, P., Jimenez, R., Juvela, M., & Nordlund, Å. 2004a, ApJ, 604, L49
Padoan, P., Jimenez, R., Nordlund, Å., & Boldyrev, S. 2004b, Physical Review Letters, 92, 191102
Ridge, N. A., et al. 2006, AJ, 131, 2921
Stanimirovic, S., Staveley-Smith, L., Dickey, J. M., Sault, R. J., & Snowden, S. L. 1999, MNRAS, 302, 417